

AD-A173 715

TURBULENT BOUNDARY LAYER INDUCED BY THERMAL PRECURSOR

1/1

(U) AEROSPACE CORP EL SEGUNDO CA AEROPHYSICS LAB

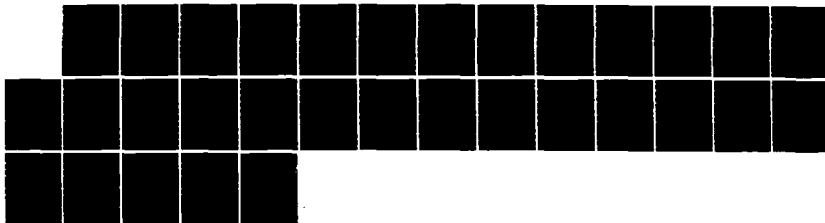
H MIRELS 20 JUN 86 TR-0086(6785)-2 SD-TR-86-38

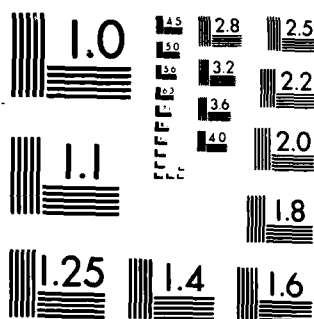
UNCLASSIFIED

F04701-85-C-0086

F/G 20/4

NL





MICROCOPY RESOLUTION TEST CHART  
NATIONAL BUREAU OF STANDARDS 1963-A

12

AD-A173 715

## Turbulent Boundary Layer Induced by Thermal Precursor

H. MIRELS  
✓Aerophysics Laboratory  
Laboratory Operations  
The Aerospace Corporation  
El Segundo, Ca 90245

20 June 1986

APPROVED FOR PUBLIC RELEASE;  
DISTRIBUTION UNLIMITED

DTIC  
ELECTE  
NOV 05 1986  
S E D

DTIC FILE COPY

Prepared for  
DEFENSE NUCLEAR AGENCY  
Washington, D.C.

SPACE DIVISION  
AIR FORCE SYSTEMS COMMAND  
Los Angeles Air Force Station  
P.O. Box 92960, Worldway Postal Center  
Los Angeles, Calif. 90009-2960


009575 SH

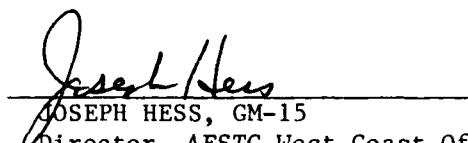
This report was submitted by The Aerospace Corporation, El Segundo, CA 90245, under Contract No. F04701-85-C-0086 with the Space Division, P. O. Box 92960, Worldway Postal Center, Los Angeles, CA 90009. It was reviewed and approved for The Aerospace Corporation by W. P. Thompson, Director, Aerophysics Laboratory.

Lieutenant Scott W. Levinson, SD/YNS, was the Air Force project officer.

This report has been reviewed by the Public Affairs Office (PAS) and is releasable to the National Technical Information Service (NTIS). At NTIS, it will be available to the general public, including foreign nationals.

This technical report has been reviewed and is approved for publication. Publication of this report does not constitute Air Force approval of the report's findings or conclusions. It is published only for the exchange and stimulation of ideas.

  
SCOTT W. LEVINSON, Lt, USAF  
MOIE Project Officer  
SD/YNS

  
JOSEPH HESS, GM-15  
Director, AFSTC West Coast Office  
AFSTC/WCO OL-AB



Unclassified

SECURITY CLASSIFICATION OF THIS PAGE(When Data Entered)

19. KEY WORDS (Continued)

20. ABSTRACT (Continued)

plate. In all cases, the maximum boundary layer thickness and minimum wall shear occur at the streamwise station  $\xi_m = \theta/\delta$  which connects a similarity solution for  $\xi < \xi_m$  with a similarity solution for  $\xi > \xi_m$ . A similar result is deduced for the corresponding case of a laminar boundary layer, with  $\xi_m = 7/9$  and 0.384 for the incompressible turbulent and laminar cases, respectively.

Unclassified

SECURITY CLASSIFICATION OF THIS PAGE(When Data Entered)

# CONTENTS

I.	INTRODUCTION.....	5
II.	THEORY.....	7
	A. Flow Description.....	7
	B. Solution of Boundary Layer Equations.....	9
	C. Laminar Boundary Layer Case.....	15
III.	CONCLUDING REMARKS.....	17
APPENDICES		
	A. Characteristic Boundary Layer Thicknesses.....	23
	B. Related Boundary Layers.....	25
	C. Comparison with Reference 12.....	27
	REFERENCES.....	29

Accession For	
NTIS GRA&I	<input checked="" type="checkbox"/>
DTIC TAB	<input type="checkbox"/>
Unannounced	<input type="checkbox"/>
Justification	
By _____	
Distribution/	
Availability Codes	
Dist	Avail and/or Special
A-1	



## FIGURES

1	Interaction of moving shock with semi-infinite thin-thermal-layer.....	6
2.	Boundary layer in thermal precursor region.....	8
3.	Simplified model for thermal precursor flow field .....	10
4.	Flow field associated with passage of shock over semi-infinite flat plate.....	18
5.	Wall boundary layer in shock tube for case of thin expansion wave and ideal (unperturbed) centerline flow.....	19
6.	Flow field associated with impulsive start of fluid motion over a semi-infinite flat plate.....	20
7.	Numerical estimate for local surface shear and boundary layer thickness associated with shock passage over semi-infinite plate for case of air with $M_s = 1.58$ , $T_1 = 290$ K, $p_1 = 1$ atm, and $x_s = 419.3$ cm.....	21



## I. INTRODUCTION

Passage of a shock moving with uniform velocity over a thin layer of heated fluid results in the formation of a thermal precursor (Fig. 1). This interaction was studied analytically in Ref. 1 and experimentally, for weak shocks, in Refs. 2 and 3. More recently, an inviscid numerical code was used<sup>4</sup> to evaluate thermal precursor flow fields. An analytical model developed in Ref. 5 yields results that are in approximate agreement with numerical examples reported in Ref. 4.

The present study provides an estimate for the turbulent boundary layer development within the precursor region. Results from Refs. 4 and 5 are used as a guide to define the inviscid flow external to the boundary layer. The turbulent boundary layer within the precursor is then evaluated using an unsteady momentum integral formulation. Boundary layer thickness parameters are defined in Appendix A. Related problems, namely, the turbulent boundary layer induced by passage of a shock wave over a semi-infinite plate, the turbulent wall boundary layer induced in a shock tube, and the turbulent boundary layer induced by the impulsive motion of a semi-infinite plate, are discussed in Appendices B and C.

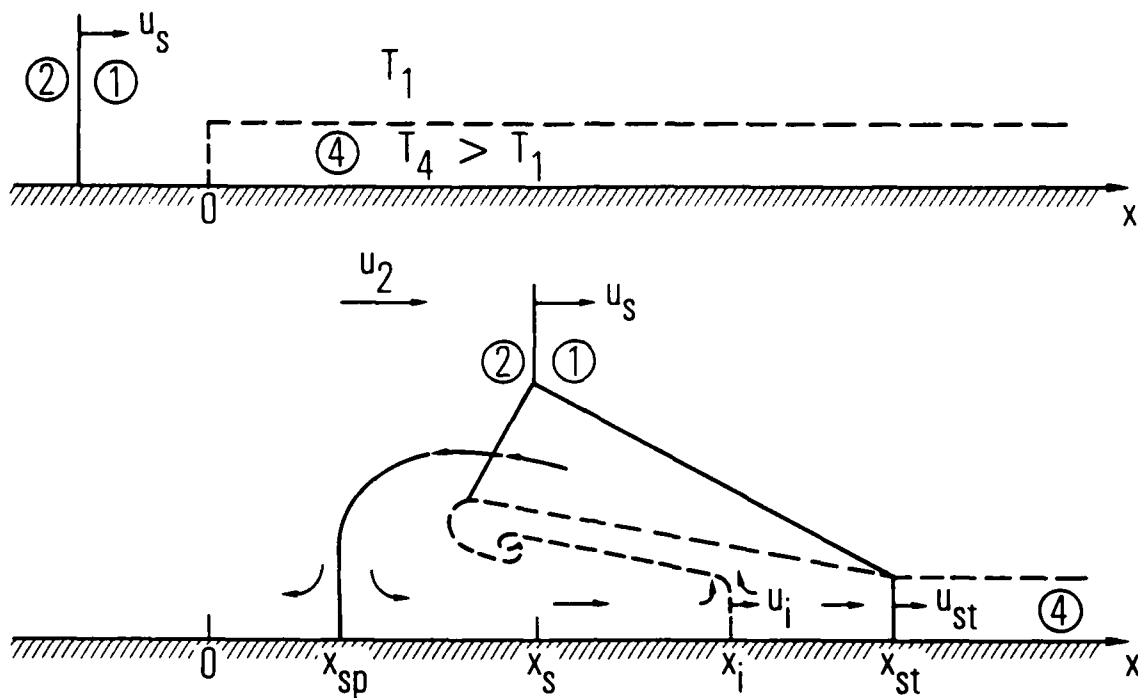


Fig. 1. Interaction of moving shock with semi-infinite thin-thermal-layer

## II. THEORY

The thermal precursor flow field is described. A solution is then presented for the turbulent boundary layer induced within the precursor.

### A. FLOW DESCRIPTION

The inviscid thermal precursor flow field, illustrated in Fig. 1, occurs when the stagnation pressure downstream of a shock of strength  $M_4 = u_s/a_4$  in region 4 is less than the static pressure downstream of the incident shock  $M_s = u_s/a_1$  in region 1. In the latter case, a portion of the fluid in region 2 moves forward and drives a shock in the thermal layer with velocity  $u_{st} > u_s$ . The interface between the fluids from regions 1 and 4 is indicated by a dashed line in Fig. 1. The quantities  $x_{sp}$ ,  $x_i$ , and  $x_{st}$  in Fig. 1 denote, respectively, the location of a local wall stagnation point, the interface location at the wall, and the location of the shock wave within the thermal layer. The incident shock location is denoted  $x_s$ . The velocities corresponding to  $x_{sp}$ ,  $x_i$ , and  $x_{st}$  are denoted  $u_{sp}$ ,  $u_i$ , and  $u_{st}$ , respectively. The results of Ref. 4 indicate that, after an initial transient, these velocities tend to constant values.

The boundary layer within the precursor region is illustrated in Fig. 2. The dashed line again denotes the interface between fluids from regions 1 and 4. The boundary layer in the intervals  $x_i < x < x_{st}$  and  $x < 0$  can be reduced to a steady state by considering coordinate systems wherein the thermal layer shock and the free stream shock are stationary, respectively. The latter are termed "shock induced boundary layers" in Fig. 2 and can be accurately evaluated (e.g., Ref. 6). The boundary layer in the region  $0 < x < x_i$  cannot be reduced to a steady state. The solution is complicated by the presence of the interface within the boundary layer. A solution for these regions is given in the next section. A similar boundary layer is associated with the impulsive motion of a semi-infinite plate,<sup>7</sup> with a shock tube wall,<sup>8</sup> and with shock passage over a semi-infinite plate.<sup>9</sup> References 7 to 9 consider laminar boundary layers. The corresponding unsteady turbulent boundary layer problems are discussed in Appendix B.

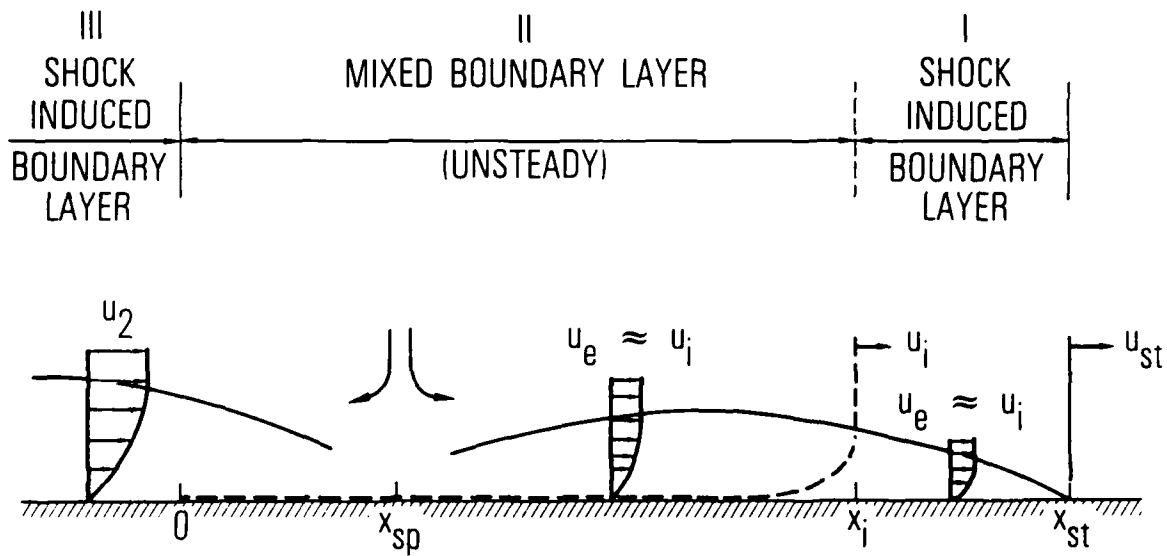


Fig. 2. Boundary layer in thermal precursor region

## B. SOLUTION OF BOUNDARY LAYER EQUATIONS

The present flow model is indicated in Fig. 3. It is assumed that each of the streamwise stations  $x_s$ ,  $x_{sp}$ ,  $x_1$ , and  $x_{st}$  moves with constant velocity. The separation between  $x_s$  and  $x_{sp}$  is ignored (Fig. 3a). The latter assumption is used to simplify the solution for the initial portion of region III and does not affect regions I and II. The flow field, at time  $t = t'$ , is illustrated in Fig. 3b. The free stream velocity in regions I and II is assumed to equal the interface velocity  $u_i$ , in approximate accord with the results of Refs. 4 and 5. The streamwise variation of fluid properties of state, external to the boundary layer in regions I and II, is ignored. The effect of the latter assumption is discussed in "Concluding Remarks."

The momentum integral equation for each of the regions I, II, and III, in Fig. 3, can be expressed in the form<sup>10</sup>

$$\frac{1}{u_e} \frac{\partial \delta^{**}}{\partial t} + \frac{\partial \theta}{\partial x} = \frac{\tau_w}{\rho_e u_e^2} \quad (1)$$

where  $\delta^{**}$  and  $\theta$  are as defined in Appendix A. Wall shear is related to the local boundary layer thickness  $\delta$  by the Blasius relation<sup>6</sup>

$$\frac{C_f}{2} = \frac{\tau_w}{\rho_e u_e^2} = 0.0225 \frac{\rho_m}{\rho_e} \left( \frac{v_m}{u_e \delta} \right)^{1/4} \quad (2)$$

Here, state properties are based on a mean temperature

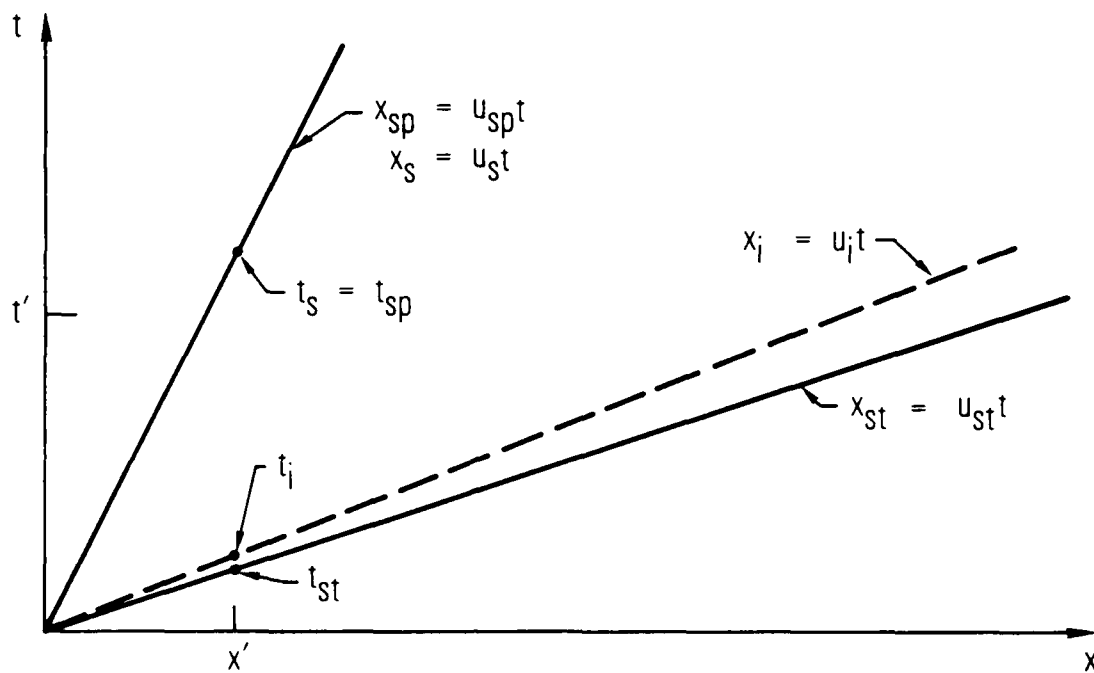
$$\frac{T_m}{T_e} = 0.5 \left( \frac{T_w}{T_e} + 1 \right) + 0.22 \left( \frac{T_r}{T_e} - 1 \right) \quad (3)$$

where  $T_w$  and  $T_r$  denote wall and recovery temperatures, respectively. (See Appendix A.)

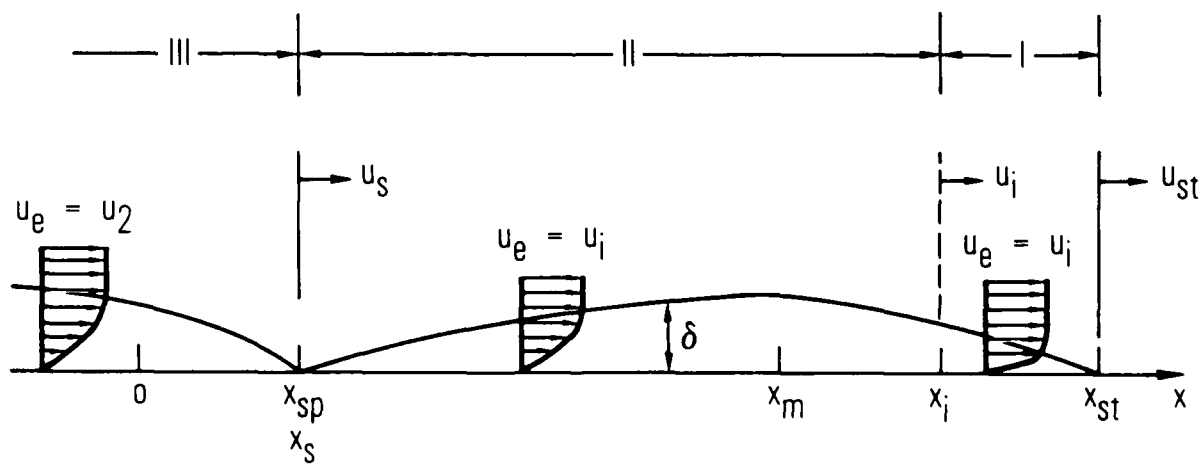
We further assume that  $\delta^{**}/\delta$  and  $\theta$ , do not vary with  $x$  or  $t$  in each of the regions of interest.

Equations (1) and (2) can then be combined to yield

$$\frac{\partial \delta^{5/4}}{\partial t} + u_e \frac{\theta}{\delta^{**}} \frac{\partial \delta^{5/4}}{\partial x} = A \quad (4a)$$



(a) INTERFACE TRAJECTORIES



(b) BOUNDARY LAYER AT TIME  $t = t'$

Fig. 3. Simplified model for thermal precursor flow field

where

$$A = 0.02813 \frac{\delta}{\delta^{**}} \frac{\rho_m}{\rho_e} v_m^{1/4} u_e^{3/4} \quad (4b)$$

Regions I and II and region III are treated separately.

# 1. Regions I and II

The independent variables are expressed in similarity form,

$$\xi = x/x_i \quad \tau = t \quad (5a)$$

where  $x_i = u_i t$ . Note  $\xi_{sp} = u_{sp}/u_i$ ,  $\xi_i = 1$ , and  $\xi_{st} = u_{st}/u_i$ .

Also, let

$$\delta^{5/4} = \tau f(\xi) \quad (5b)$$

Equation (4a) becomes

$$(\xi^* - \xi) (df/d\xi) + f = A \quad (6a)$$

where

$$\xi^* = \theta/\delta^{**} \quad (6b)$$

The boundary layer thickness  $\delta$  has been assumed to be zero at  $\xi_{sp}$  and  $\xi_{st}$  (Fig. 3b). The boundary conditions are then

$$f(\xi_{sp}) = 0 \quad (7a)$$

$$f(\xi_{st}) = 0 \quad (7b)$$

Since streamwise variations of  $A$  and  $\xi^*$  are being neglected, Eq. (6a) can be integrated to yield

$$f = A + C (\xi - \xi^*) \quad (8)$$

where  $C$  is a constant.

The boundary conditions [Eqs. (7a) and (7b)] provide two separate values for  $C$ . The resulting two solutions for  $f$  can be joined at station  $\xi_m$  such that  $f$ , and therefore  $\delta$  are continuous at  $\xi_m$ . The result is

$$\frac{f}{A} = \frac{\xi_{st} - \xi}{\xi_{st} - \xi_m} \quad \xi < \xi < \xi_{st} \quad (9a)$$

$$= \frac{\xi - \xi_{sp}}{\xi_m - \xi_{sp}} \quad \xi_{sp} < \xi < \xi_m \quad (9b)$$

where

$$\begin{aligned} \xi_m &= \xi^* \equiv \theta/\delta^{**} \\ &= 7/9 \quad \text{Incompressible flow} \end{aligned} \quad (9c)$$



The ability to satisfy the boundary conditions at  $\xi_{sp}$  and  $\xi_{st}$  and match at  $\xi_m = \xi^*$  is a consequence of the fact that  $\xi^*$  is a singular point of Eq.

(6a). The boundary layer thickness is a maximum at  $\xi_m$  (Fig. 3). The surface shear is a minimum at that station.

The boundary layer thickness and local surface shear coefficient can be expressed in physical variables. The result, for  $\xi_{sp} < \xi < \xi_m$ , is

$$\left(\frac{\theta/\delta}{7/72}\right)^{4/5} \delta = \frac{0.3707 \phi}{[1 - (\xi_{sp}/\xi_m)]^{4/5}} (x - u_{sp}t)^{4/5} \left(\frac{v_e}{u_e}\right)^{1/5} \quad (10a)$$

$$\left(\frac{7/72}{\theta/\delta}\right)^{1/5} c_f = \frac{0.05767 \phi}{[1 - (\xi_{sp}/\xi_m)]^{-1/5}} (x - u_{sp}t)^{-1/5} \left(\frac{v_e}{u_e}\right)^{1/5} \quad (10b)$$

and for  $\xi_m < \xi < \xi_{st}$

$$\left(\frac{\theta/\delta}{7/72}\right)^{4/5} \delta = \frac{0.3707 \phi}{[(\xi_{st}/\xi_m) - 1]^{4/5}} (u_{st}t - x)^{4/5} \left(\frac{v_e}{u_e}\right)^{1/5} \quad (11a)$$

$$\left(\frac{7/72}{\theta/\delta}\right)^{1/5} c_f = \frac{0.05767 \phi}{[(\xi_{st}/\xi_m) - 1]^{-1/5}} (u_{st}t - x)^{-1/5} \left(\frac{v_e}{u_e}\right)^{1/5} \quad (11b)$$

where

$$\phi = (\rho_m/\rho_e)^{4/5} (v_m/v_e)^{1/5}$$

The ratio  $\theta/\delta$  in Eqs. (10) and (11) has been normalized by the value for incompressible flow. The solution, however, is not limited to incompressible flow.

In the limit  $\xi_{sp} = 0$ , Eqs. (10a) and (10b) correspond to the steady-state solution for a turbulent boundary layer on a semi-infinite flat plate.<sup>11</sup> When  $\xi_{sp} \neq 0$ , Eqs. (10a) and (10b) account for streamwise motion of the boundary condition  $\delta = 0$  at  $x_{sp}$ . Equations (11a) and (11b) correspond to the solution for a turbulent boundary layer behind a shock moving with uniform velocity.<sup>6</sup> The solution is accurate, in region I, if the appropriate free stream conditions are used.

## 2. Region III

The boundary layer in region III corresponds to the boundary layer behind the incident shock which moves with velocity  $u_s = x_s/t$ . Let subscript 2 denote free stream conditions behind the incident shock and define  $\bar{\xi} = x/u_2 t$ . A derivation, similar to that for Eqs. (11a) and (11b) yields for  $\bar{\xi} < \bar{\xi}_s$

$$\left(\frac{\theta/\delta}{7/72}\right)^{4/5} \delta = \frac{0.3707 \phi}{[(\bar{\xi}_s/\xi_2^*) - 1]^{4/5}} (u_s t - x)^{4/5} \left(\frac{v_2}{u_2}\right)^{1/5} \quad (12a)$$

$$\left(\frac{7/72}{\theta/\delta}\right)^{1/5} C_f = \frac{0.05767 \phi}{[(\bar{\xi}_s/\xi_2^*) - 1]^{-1/5}} (u_s t - x)^{-1/5} \left(\frac{v_2}{u_2}\right)^{1/5} \quad (12b)$$

where  $\phi = (\rho_m/\rho_2)^{4/5} (v_m/v_2)^{1/5}$ ,  $\xi_2^* = (\theta/\delta^{**})_2$  and

$$\bar{\xi}_s = u_s/u_2 = [1 - (\rho_1/\rho_2)]^{-1} \quad (12c)$$

Here,  $\rho_2/\rho_1$  is the density ratio across the incident shock. Equations (12a)-(c) are applicable in the region  $x < 0$  and, for the case  $u_s = u_{sp}$  in the region  $0 < x < x_{sp}$ .

## 3. Time Dependence at Fixed Station

Equations (10) through (12) can be put into a form which is convenient for evaluating boundary layer properties at a fixed station (e.g.,  $x'$  in Fig. 3a). Assume that the interaction starts at time  $t = 0$  (Fig. 3a) and let  $t_s$ ,

$t_{sp}$ ,  $t_i$ , and  $t_{st}$  denote interface arrival times at  $x'$ . Boundary layer properties at station  $x'$  are found from Eqs. (10) through (12) by use of the following substitutions:

$$\frac{1}{u_e} \frac{x - u_{sp}t}{1 - (\xi_{sp}/\xi_m)} = \frac{(t_{sp} - t)t_i}{t_{sp} - t_m} \quad (13a)$$

$$\frac{1}{u_e} \frac{u_{st}t - x}{(\xi_{st}/\xi_m) - 1} = \frac{(t - t_{st})t_i}{t_m - t_{st}} \quad (13b)$$

$$\frac{1}{u_2} \frac{u_s t - x}{(\bar{\xi}_s/\xi_2^*) - 1} = \frac{t - t_s}{(\bar{\xi}_2^*)^{-1} - (\bar{\xi}_s)^{-1}} \quad (13c)$$

where  $t_m = t_i/\xi_m$ . It is clear from Eqs. (13a) and (13b) that the boundary layer solution is continuous at time  $t = t_m$ .

#### C. LAMINAR BOUNDARY LAYER CASE

The present procedure can be used to treat the case of a laminar boundary layer induced by a thermal precursor and related laminar problems.<sup>7-9</sup> In particular, the quantity  $\delta^{5/4}$  in Eqs. (4a) and (5b) is replaced by  $\delta^2$  and the constant A is expressed as

$$A = 2 \tau_w \delta / (\rho_e u_e^2) \quad (14)$$

The solution for  $f = \delta^2/\tau$  is then given by Eq. (9). The maximum boundary layer thickness occurs at

$$\begin{aligned} \xi_m &= \theta/\delta^{**} \\ &= 0.384 \text{ (incompressible}^{11}) \end{aligned} \quad (15)$$

which may be compared with the value  $\xi_m = 7/9$  for an incompressible turbulent boundary layer.

### III. CONCLUDING REMARKS

A solution has been presented for the turbulent boundary layer within a thermal precursor. The solution is limited because differences in fluid state properties between regions I and II have not been taken into account. An improved theory can be developed by the piecewise application of Eq. (8) in regions  $x_{sp} < x < x_m$ ,  $x_m < x < x_i$ , and  $x_i < x < x_{st}$  wherein the boundary condition  $\delta = 0$  is satisfied at  $x_{sp}$  and  $x_{st}$  and  $\delta$  is continuous at  $x_m$  and  $x_i$ . This approach does not appear warranted without an improved model for the boundary layer in region  $x_m < x < x_i$ .

The numerical thermal precursor solutions of Ref. 4 indicate that, after an initial transient,  $u_1 = u_{st}$ . Thus the separation distance  $x_{st} - x_i$  remains constant. The fixed separation  $x_{st} - x_i$  is a consequence of the fact that the fluid which crosses the shock in the thermal layer is not constrained to remain between  $x_{st}$  and  $x_i$  (as in a shock tube), but is ejected from the wall region near  $x_i$ . The flow is then similar to supersonic flow (of the heated layer gas) over a blunt body (cold precursor gas).<sup>5</sup> Thus, after long times  $x_{st} - x_i$  is small compared with  $x_{st} - x_{sp}$ . Hence region I is small compared with region II. In this case (i.e.,  $\xi_{st} \rightarrow \xi_i$ ), the turbulent boundary layer in the precursor can be estimated from Eqs. (10) and (11) by using free-stream properties from region II in each of these equations.

The boundary layer behind a shock moving over a semi-infinite plate, the shock tube wall boundary layer, and the boundary layer associated with impulsive fluid motion over a semi-infinite plate are illustrated in Figs. 4 through 6, respectively. These flows represent special cases of Eqs. (10) and (11) and are discussed in Appendix B. Numerical results for the shock-induced turbulent boundary layer on a semi-infinite plate are given in Ref. 12 and compared with the present model in Appendix C. Reference 12 presents surface shear and boundary layer thickness for the case of standard air with  $M_s = 1.58$  and  $x_s = 419.3$  cm. These results, based on a numerical mixing length model, are given in Fig. 7. For this case, the present model predicts that the maximum boundary layer thickness and the minimum surface shear occur

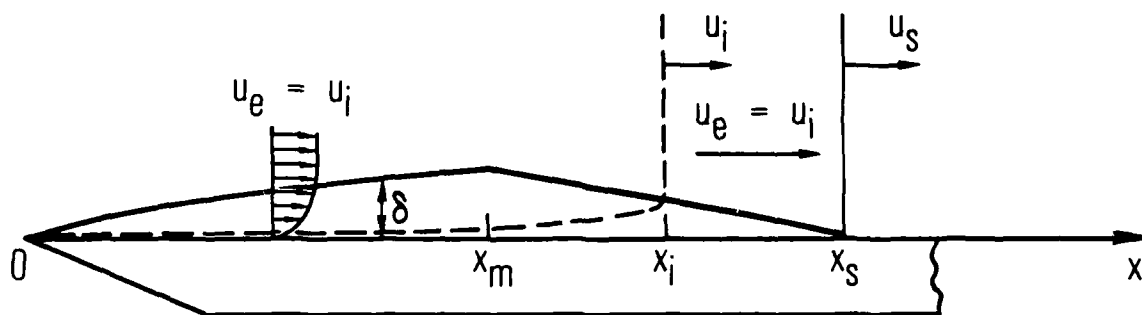


Fig. 4. Flow field associated with passage of shock over semi-infinite flat plate. Dashed line denotes particles that were at  $x = 0$  at time  $t = 0$

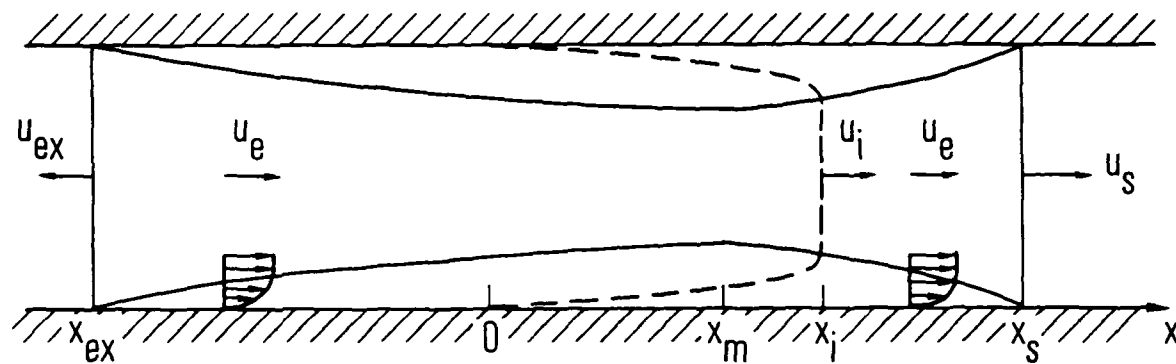


Fig. 5. Wall boundary layer in shock tube for case of thin expansion wave and ideal (unperturbed) centerline flow. Dashed line denotes particles at diaphragm location ( $x = 0$ ) at time  $t = 0$

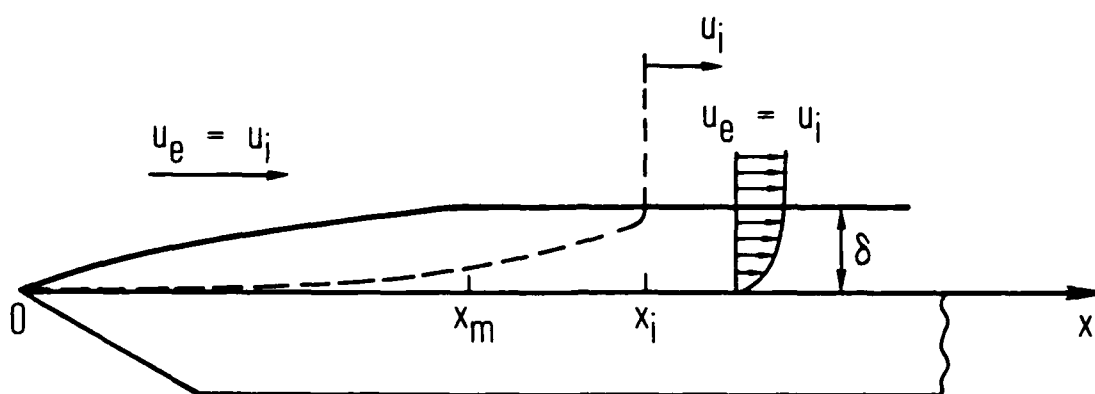


Fig. 6. Flow field associated with impulsive start of fluid motion over a semi-infinite flat plate. Dashed line denotes particles that were at  $x = 0$  at time  $t = 0$

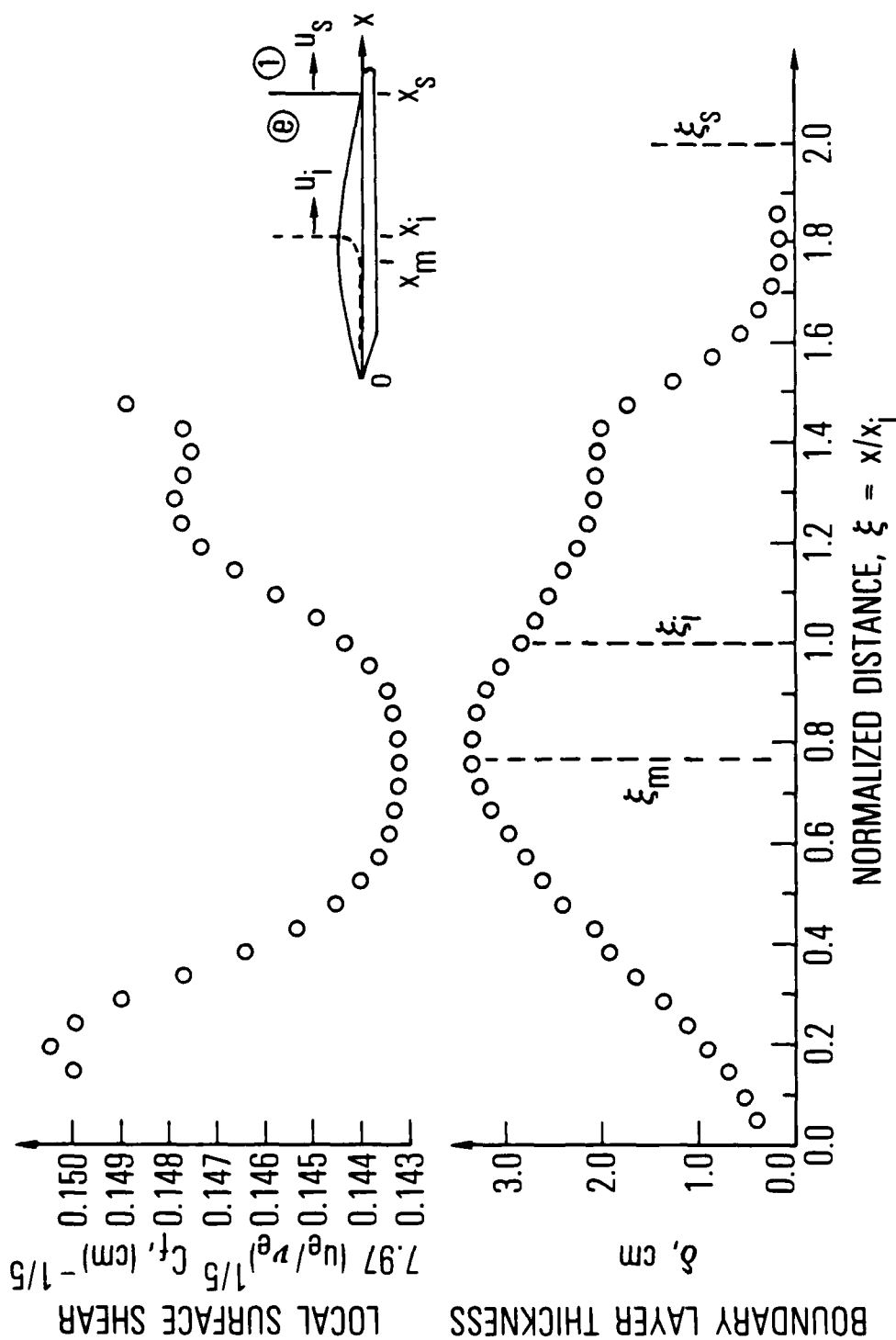


Fig. 7 Numerical estimate<sup>12</sup> for local surface shear and boundary layer thickness associated with shock passage over semi-infinite plate for case of air with  $M_g = 1.58$ ,  $T_1 = 290$  K,  $p_1 = 1$  atm, and  $x_g = 419.3$  cm. For present case,  $\xi_g = 2$ ,  $\xi_i = 1$ , and  $\xi_m = \theta/\delta = 0.772$ .



at  $\xi_m \equiv \theta/\delta^{**} = 0.772$ . This prediction is seen to be in good agreement with the numerical results of Ref. 12.

## APPENDIX A

### CHARACTERISTIC BOUNDARY LAYER THICKNESSES

Let subscript e denote local free stream properties in a wall fixed coordinate system. Boundary layer defect thicknesses are then

$$\delta^*/\delta = \int_0^1 [1 - (\rho u / \rho_e u_e)] dy/\delta \quad (A-1a)$$

$$\theta/\delta = \int_0^1 (\rho u / \rho_e u_e) [1 - (u/u_e)] dy/\delta \quad (A-1b)$$

$$\delta^{**}/\delta = \int_0^1 (\rho/\rho_e) [1 - (u/u_e)] dy/\delta \quad (A-1c)$$

where  $\delta^*$  and  $\theta$  are displacement and momentum thicknesses, respectively. The quantity  $\delta^{**}$  appears in Eq. (1) and reduces to  $\delta^*$  for the case of an incompressible fluid.

Equations (A-1a)-(c) can be evaluated for a turbulent boundary layer if velocity and density profiles are known. A suitable choice is<sup>6</sup>

$$u/u_e = (y/\delta)^{1/7} \quad (A-2a)$$

$$\frac{\rho_e}{\rho} = \frac{T_w}{T_e} \left[ 1 + b \left( \frac{u}{u_e} \right) - c \left( \frac{u}{u_e} \right)^2 \right] \quad (A-2b)$$

where

$$b = (T_r/T_w) - 1$$

$$c = [(T_r/T_e) - 1] (T_e/T_w)$$

$$T_r/T_e = 1 + [(\gamma - 1)/2] r(o) M_e^2$$

Here subscripts w and r denote wall and recovery values, respectively. The recovery factor  $r(0)$  equals 0.90 for air.

For the case of an incompressible fluid, Eqs. (A-1a)-(c) become

$$\delta^*/\delta = \delta^{**}/\delta = 1/8 \quad (A-3a)$$

$$\theta/\delta = 7/72 \quad (A-3b)$$

Equation (A-3b) has been used in the body of the report to normalize  $\theta/\delta$ .

## APPENDIX B

### RELATED BOUNDARY LAYERS

The turbulent boundary layers induced by passage of a shock over a semi-infinite flat plate, by shock tube flow and by the impulsive start of fluid motion over a semi-infinite flat plate, have features that are similar to the boundary layer in a thermal precursor. These boundary layers are now discussed.

The flow associated with shock passage over a semi-infinite plate is illustrated in Fig. 4. The dashed line indicates particles that were located at  $x = 0$  at time  $t = 0$ . A solution for the laminar boundary layer case, in the limit  $M_s \rightarrow 1$ , is presented in Ref. 9, in which unsteady two-dimensional laminar boundary layer equations were considered. The flow in Fig. 4 is similar to the flow in Fig. 3b with  $u_{sp} = 0$ . Hence, a momentum integral solution for the turbulent boundary layer case leads to Eqs. (10) and (11) with  $\xi_{sp} = u_{sp} = 0$  in Eqs. (10a) and (10b). The flow in region  $0 < x < x_m$  corresponds to a steady flow over a semi-infinite flat plate. The flow in region  $x_m < x < x_s$  corresponds to the boundary layer induced by a moving shock wave. Station  $x_m$  (i.e.,  $\xi_m = \theta/\delta^{**}$ ) represents the station at which  $\delta$  is matched for these two flows and is a maximum. In this case, the assumption of uniform free-stream properties, external to the boundary layer, is exactly satisfied.

The wall boundary layer induced in a shock tube is illustrated in Fig. 5. A finite difference solution for the boundary layer in region  $0 < x < x_1$  was presented in Ref. 8. for the case of laminar flow. Equations (10) and (11) can be used to estimate the turbulent boundary layer everywhere in the shock tube if the expansion wave thickness is neglected (as illustrated in Fig. 5) and if fluid property differences between the driver gas and the driven gas are neglected. The boundary layer in region  $x_{ex} < x < x_m$  is found from Eq. (10) with  $u_{sp}$  and  $\xi_{sp}$  replaced by  $u_{ex}$  and  $\xi_{ex} \equiv x_{ex}/x_1$ , respec-

tively. Note that  $u_{ex}$  and  $\xi_{ex}$  are both negative. The boundary layer in region  $x_m < x < x_s$  is obtained from Eq. (11). It is seen that the maximum value of  $\delta$  again occurs at  $\xi_m = \theta/\delta^{**}$ .

The flow associated with impulsive motion of flow, over a semi-infinite flat plate, is illustrated in Fig. 6. The flow is assumed to be impulsively started at time  $t = 0$ . The dashed line represents particles that were at  $x = 0$  at time  $t = 0$ . The laminar case, discussed in Ref. 7, contains a momentum integral solution and a discussion of the singular nature of the full laminar boundary layer equations. A momentum integral solution for the turbulent case yields Eqs. (10a) and (10b) with  $\xi_{sp} = u_{sp} = 0$ , for  $0 < x < x_m$ . Hence, here too, the flow is equivalent to steady flow over a semi-infinite plate. For  $x > x_m$ , the boundary layer thickness and shear are time dependent but do not vary with  $x$ . Boundary layer properties are found by evaluating Eqs. (10a) and (10b) with  $\xi_{sp} = u_{sp} = 0$ , at  $x = x_m = (\theta/\delta^{**})(u_e t)$ . The boundary layer for  $x > x_m$  is the turbulent analog for the laminar Rayleigh problem<sup>11</sup> wherein an infinite plate is set into motion at time  $t = 0$ . The present procedure, to match at  $x_m$ , is similar to the approach used in Ref. 7 for the laminar case.

In all of these cases, as in the case of the thermal precursor, the maximum value of  $\delta$  and the minimum value of wall shear occur at  $\xi_m = \theta/\delta^{**}$ . As previously noted, the latter represents a singular point which joins the similarity solution for  $\xi < \xi_m$  to the similarity solution for  $\xi > \xi_m$  and is in accord with the theory of Stewartson.<sup>7</sup>

## APPENDIX C

### COMPARISON WITH REFERENCE 12

Numerical turbulent boundary layer results are reported in Ref. 12 which provide the variation of surface shear and boundary layer thickness behind a shock moving over a semi-infinite plate (Fig. 4). A mixing length model was used and finite difference calculations were performed. The results of Ref. 12 are compared herein with the present model.

The local shear and boundary layer thickness variation, from Ref. 12, is given in Fig. 7. These data are for the case of air and  $M_g = 1.58$ ,  $T_1 = 290$  K, and  $P_1 = 1$  atmosphere. The data represent values at the instant of time when the shock is at  $x_g = 419.3$  cm. For this case  $\delta^*/\delta = 0.1330$ ,  $\theta/\delta = 0.09916$ ,  $\delta^{**}/\delta = 0.12845$ ,  $\xi_s = 2.0$ ,  $\xi_1 = 1.0$ , and  $\xi_m \equiv \theta/\delta^{**} = 0.772$ . In the vicinity of  $\xi = \xi_m$ , the numerical results for  $\delta$  and  $C_f$  in Ref. 12 are approximately equal to 1.8 and 0.8 times the values deduced herein, respectively.

The station at which surface shear is a minimum and boundary layer thickness is a maximum is of primary interest. The present model predicts this location to be at  $\xi_m = 0.772$ , which is included in Fig. 7. It is seen that this prediction is in close agreement with the numerical results of Ref. 12. This agreement tends to confirm the present model.

#### REFERENCES

1. Hess, R. V., "Interaction of Moving Shocks and Hot Layers," NACA TN 4002, 1957.
2. Griffith, W. C., "Interaction of a Shock Wave with a Thermal Boundary Layer," J. Aero. Sci., Jan. 1956.
3. Gion, E. J., "Plane Shock Interacting with Thermal Layer," Physics of Fluids, 20, No. 4, April 1977.
4. Schneyer, G. P., and Wilkins, D. E., "Thermal Layer-Shock Interaction (Precursor) Simulation Data Book," S-Cubed Report No. SSS-R-84-6584, Mar. 1984.
5. Mirels, H., Interaction of Moving Shock With Thin Stationary Thermal Layer, The Aerospace Corporation, TR-0084A(5785)-1 (1985).
6. Mirels, H., "Turbulent Boundary Layer Behind Constant Velocity Shock Including Wall Blowing Effects," AIAA J. 22, Aug. 1984.
7. Stewartson, K., "On The Impulsive Motion of a Flat Plate in a Viscous Fluid," Quart. J. Mech. and Appl. Math., Vol. IV, Pt. 2 (1951).
8. Ban, S. D. and Kuerti, G., "The Interaction Region in the Boundary Layer of a Shock Tube", J. Fluid. Mech. 38, 109-125 (1969).
9. Lam, S. H. and Crocco, L., "Note On The Shock Induced Unsteady Laminar Boundary Layer on a Semi-Infinite Flat Plate," J. Aero/Space Sci., Jan 1959, p. 54.
10. Rosenhead, L., Laminar Boundary Layers, Oxford Univ. Press (1963), p. 207.
11. Schlichting, H., Boundary Layer Theory, McGraw Hill (1960) pp. 72, 242, 537.
12. Bennett, B. C., Abbett, M. J. and Wolf, C. J., "Viscous Effects On Blast Wave Flowfields", Acurex Final Rept FR-85-11/ATD, December, 1984.

## LABORATORY OPERATIONS

The Aerospace Corporation functions as an "architect-engineer" for national security projects, specializing in advanced military space systems. Providing research support, the corporation's Laboratory Operations conducts experimental and theoretical investigations that focus on the application of scientific and technical advances to such systems. Vital to the success of these investigations is the technical staff's wide-ranging expertise and its ability to stay current with new developments. This expertise is enhanced by a research program aimed at dealing with the many problems associated with rapidly evolving space systems. Contributing their capabilities to the research effort are these individual laboratories:

Aerophysics Laboratory: Launch vehicle and reentry fluid mechanics, heat transfer and flight dynamics; chemical and electric propulsion, propellant chemistry, chemical dynamics, environmental chemistry, trace detection; spacecraft structural mechanics, contamination, thermal and structural control; high temperature thermomechanics, gas kinetics and radiation; cw and pulsed chemical and excimer laser development including chemical kinetics, spectroscopy, optical resonators, beam control, atmospheric propagation, laser effects and countermeasures.

Chemistry and Physics Laboratory: Atmospheric chemical reactions, atmospheric optics, light scattering, state-specific chemical reactions and radiative signatures of missile plumes, sensor out-of-field-of-view rejection, applied laser spectroscopy, laser chemistry, laser optoelectronics, solar cell physics, battery electrochemistry, space vacuum and radiation effects on materials, lubrication and surface phenomena, thermionic emission, photo-sensitive materials and detectors, atomic frequency standards, and environmental chemistry.

Computer Science Laboratory: Program verification, program translation, performance-sensitive system design, distributed architectures for spaceborne computers, fault-tolerant computer systems, artificial intelligence, micro-electronics applications, communication protocols, and computer security.

Electronics Research Laboratory: Microelectronics, solid-state device physics, compound semiconductors, radiation hardening; electro-optics, quantum electronics, solid-state lasers, optical propagation and communications; microwave semiconductor devices, microwave/millimeter wave measurements, diagnostics and radiometry, microwave/millimeter wave thermionic devices; atomic time and frequency standards; antennas, rf systems, electromagnetic propagation phenomena, space communication systems.

Materials Sciences Laboratory: Development of new materials: metals, alloys, ceramics, polymers and their composites, and new forms of carbon; non-destructive evaluation, component failure analysis and reliability; fracture mechanics and stress corrosion; analysis and evaluation of materials at cryogenic and elevated temperatures as well as in space and enemy-induced environments.

Space Sciences Laboratory: Magnetospheric, auroral and cosmic ray physics, wave-particle interactions, magnetospheric plasma waves; atmospheric and ionospheric physics, density and composition of the upper atmosphere, remote sensing using atmospheric radiation; solar physics, infrared astronomy, infrared signature analysis; effects of solar activity, magnetic storms and nuclear explosions on the earth's atmosphere, ionosphere and magnetosphere; effects of electromagnetic and particulate radiations on space systems; space instrumentation.



END

12-86

DTIC